NA57 main results

G E Bruno for the NA57 Collaboration †

Dipartimento IA di Fisica dell'Università e del Politecnico di Bari and INFN, Bari, Italy

E-mail: `Giuseppe.Bruno@ba.infn.it`

Abstract. The CERN NA57 experiment was designed to study the production of strange and multi-strange particles in heavy ion collisions at SPS energies; its physics programme is essentially completed. A review of the main results is presented.

1. Introduction

The NA57 experiment at CERN was proposed [1] to study (multi-)strange baryon and anti-baryon production in Pb–Pb collisions at SPS. Its principal aim was to refine and extend the measurements of its predecessor WA97, which first measured the enhancements of hyperons and anti-hyperons in Pb–Pb collisions with respect to reference pBe collisions [2]. The observed pattern of enhancements increasing with the particle's strangeness content constituted one of the main pieces of evidence for the creation, in Pb-Pb collisions at the SPS, of a new state of matter displaying many of the predicted features of a deconfined system [3].

The main contributions of NA57 fall into three areas: hyperon enhancements, strange particle spectra, and nuclear modification factors.

2. Experimental technique

Strange particles were detected by reconstructing their weak decays into final state containing charged particles only, i.e., $\Lambda \rightarrow p\pi^-$, $\Xi^- \rightarrow \Lambda\pi^- \rightarrow p\pi^-\pi^-$, $\Omega^- \rightarrow \Lambda K^- \rightarrow p\pi^-K^-$ (and c.c. for anti-hyperons), and $K_S^0 \rightarrow \pi^-\pi^+$. The charged tracks emerging from strange particle decays were detected in a telescope made from an array of silicon pixel detectors of 5x5 cm^2 cross-section placed in an approximately uniform magnetic field; the bulk of the detectors was closely packed in approximately 30 cm length, this part being used for pattern recognition. The telescope was placed above the beam line, inclined and aligned with the lower edge of the detectors laying on a line pointing to the target. The inclination angle and the distance from the target were set so as to accept particles produced in about a unit of rapidity around mid-rapidity, with transverse momentum above a few hundred MeV/c. The selected samples of strange

† For the full author list see Appendix "Collaborations" in this volume.

and multi-strange particles after final kinematical cuts were almost background free (*noise/signal* at most a few percents).

The centrality of the collisions was determined by analysing the charged particle multiplicity measured by two stations of microstrip silicon detectors (MSD) which together sampled the pseudorapidity interval $2 < \eta < 4$. Detailed descriptions of the NA57 experimental apparatus, hyperon selection strategy and centrality determination can be found in references [4, 5].

3. Hyperon enhancements

An enhanced production of strange particles in nucleus–nucleus collisions with respect to proton–induced reactions was suggested long time ago as a possible signature of the phase transition from colour-confined hadronic matter to a quark-gluon plasma (QGP) [6]. Moreover, the magnitude of the enhancement was predicted to increase with the strangeness content of the particles. The argument being that the s and $\bar{s}$ quarks, abundantly produced in the deconfined phase, would recombine to form strange and multi-strange particles in a time much shorter than that required to produce them by successive rescattering interactions in a hadronic gas.

The enhancements are defined as the central rapidity particle yield per participant $(E = Y/ < N_{wound} >, \; Y = \int_{y_{cm}-0.5}^{y_{cm}+0.5} \mathrm{d}y \int_0^\infty \frac{\mathrm{d}N^2}{\mathrm{d}p_T \mathrm{d}y} \mathrm{d}p_T)$ relative to pBe collisions. The hyperon enhancements measured by NA57 at 40 and 158 A GeV/c are shown as a function of centrality in figure 1.
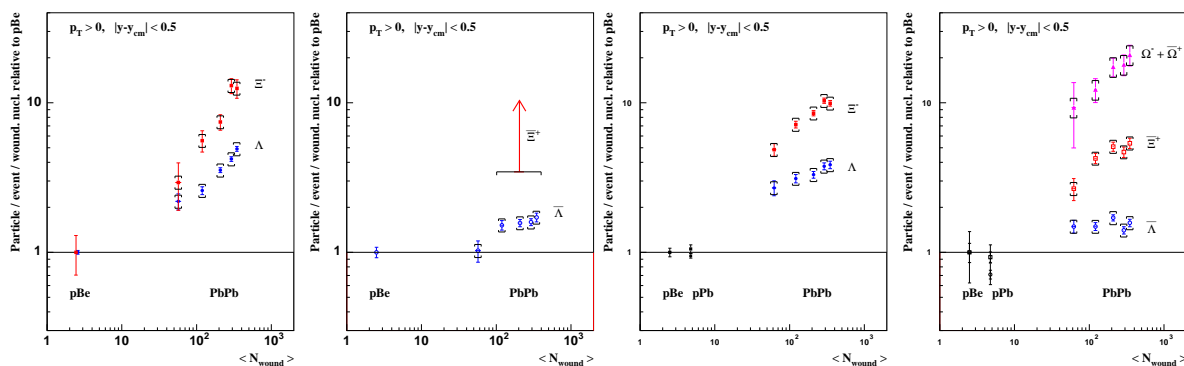

Figure 1. Hyperon enhancements as a function of the number of participants (N_{wound}) at 40 (1st and 2nd panels, ref [7]) and 158 (3rd and 4th panels, ref [4]) A GeV/c. The symbol □ shows the systematic error, the arrow in the 2nd panel indicates the lower limit to the $\overline{\Xi}^+$ enhancement in the four most central classes at 95% confidence level.

The results presented above confirm, refine and extend the study of strangeness enhancements initiated by the WA97 experiment [2]. In particular the increase of the magnitude of the enhancement with the strangeness content of the particles is confirmed, as expected in a QGP scenario [6]. The highest enhancement is measured for the triply-strange Ω hyperon and amounts to about a factor 20 in the most central class. Conventional hadronic models fail to reproduce this result. The confirmation

of the WA97 results is important in itself; however NA57 could measure the hyperon enhancement with greater detail, as a function of centrality, and of energy.

Centrality dependence A comprehensive discussion of the centrality dependence of the enhancements can be found in reference [4]. Here it is worth noting that (at 158 A GeV/c) the normalized yields for the pBe and pPb data are compatible with each other within the error limits, as expected from N_{wound} scaling. In Pb–Pb collisions the hyperon production is already significantly enhanced at N_{wound} as low as about 50, and a significant centrality dependence of the enhancements for all particles except $\overline{\Lambda}$ is observed. For the two most central classes ($\simeq 10\%$ of most central collisions) a saturation of the enhancements cannot be ruled out, in particular for Ξ^- and $\overline{\Xi}^+$. In contrast, the flatness of the $\overline{\Lambda}$ enhancement with centrality is somewhat puzzling. This could be due to some difference in the initial production mechanism, or it could be the consequence of, e.g., a centrality-dependent $\overline{\Lambda}$ absorption in a nucleon-rich environment. It is worth recalling that (i) within the NA57 acceptance $\overline{\Lambda}$ is the only strange baryon for which we observe a significantly non-flat rapidity distribution [8], and (ii) a similar behaviour of $\overline{\Lambda}$ enhancement with centrality at SPS top energy has been confirmed by NA49 [9], and it is not present, instead, at RHIC energy ($\sqrt{s_{\mathrm{NN}}} = 200$ GeV, STAR) [10].

Energy dependence We measured hyperon production in pBe and Pb–Pb collisions at 40 A GeV/c allowing us to establish that the enhancement mechanism is already effective at this energy, with the same hierarchy with the strangeness content as that observed at higher energy. For the most central collisions the enhancements are higher at 40 than at 158 GeV/c, the increase with N_{wound} is steeper at 40 than at 158 GeV/c. Similar enhancement pattern (except for the $\overline{\Lambda}$) has been measured at $\sqrt{s_{\mathrm{NN}}} = 200$ GeV/c [10].

Both dependencies put constraints on theoretical models: e.g., the *"canonical suppression"* model [11] predicts a higher enhancement at 40 GeV, but fails to reproduce the absolute amounts and the centrality dependence of the enhancements.

4. Strange particle spectra

The bulk of the kinematical distributions of the particles produced in nucleus–nucleus interactions are expected to be shaped by the superposition of two effects: the thermal motion of the particles in the *fireball* and a pressure-driven radial (for $m_{\mathrm{T}} = \sqrt{p_{\mathrm{T}}^2 + m^2}$) or longitudinal (for y) collective flow, induced by the fireball expansion. Studies of the m_{T} spectra for Λ, Ξ, Ω hyperons and K_{S}^0, measured in Pb–Pb collisions at 158 and 40 A GeV/c were presented in [12] and [13], respectively. A study of the rapidity distributions at 158 A GeV/c was presented in [8]. Here we shall concentrate on the m_{T} spectra, which were analyzed in the frame-work of the *blast-wave* model [14]. The model assumes cylindrical symmetry for an expanding fireball in local thermal equilibrium and predicts the shape of the double-differential yield $\mathrm{d}^2N/\mathrm{d}m_{\mathrm{T}}\mathrm{d}y$ for the different particle species, in terms of the kinetic freeze-out temperature T and of the radial velocity profile $\beta_{\perp}(r)$. The latter was parametrized as $\beta_{\perp}(r) = \beta_S \cdot r/R_G$, β_S being the flow velocity at the freeze-out surface and R_G the outer radius. The fit to the experimental spectra

allows us to extract T and the average transverse flow velocity $\langle\beta_\perp\rangle = 2/3 \cdot \beta_S$. The 1σ contour plot in the freeze-out parameter space is shown in figure 2 (left panel) for the most central 53% of the inelastic Pb–Pb cross section at 40 and 158 A GeV/c. More detailed analyses of the spectra [12, 13] suggested that multi-strange hyperons could possibly undergo an earlier freeze-out than singly strange particles.
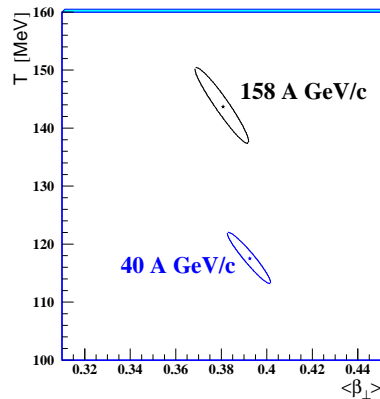

Figure 2. Contour plots in the T–$\langle\beta_\perp\rangle$ plane at the 1σ confidence level.

Similar results were reported at the SPS by the NA49 experiment [15]. NA57 has measured the m_T spectra also as a function of centrality, as shwon, e.g., in left and middle panels of figure 3. Therefore we could explore the centrality dependence of the freeze-out parameters, which can be summarized as follows: the more central the collisions the stronger the transverse collective flow and the lower the final thermal freeze-out temperature. This finding is very relevant to the question of whether observables at the SPS (e.g. the elliptic flow) can be described hydro-dynamically, as it is the case at RHIC (see [16] for a discussion).

5. Nuclear modification factors R_{CP}

At the Relativistic Heavy Ion Collider (RHIC), the central-to-peripheral nuclear modification factor

$$R_{\mathrm{CP}}(p_\mathrm{T}) = \frac{\langle N_{\mathrm{coll}}\rangle_\mathrm{P}}{\langle N_{\mathrm{coll}}\rangle_\mathrm{C}} \times \frac{\mathrm{d}^2 N^\mathrm{C}_{\mathrm{AA}}/\mathrm{d}p_\mathrm{T}\mathrm{d}y}{\mathrm{d}^2 N^\mathrm{P}_{\mathrm{AA}}/\mathrm{d}p_\mathrm{T}\mathrm{d}y}$$

measured for a large variety of particles has proved to be a powerful tool for the study of parton propagation in the dense QCD medium expected to be formed in nucleus–nucleus collisions (see, e.g., [17]). At SPS energies, only π^0 R_{CP} measurements were available [18] prior to NA57; we reported the first results on the particle species dependence (unidentified negatively charged hadrons, K^0_S, Λ, and $\overline{\Lambda}$) in [19]. Figure 4 (left panel) shows the results for 0–5%/40–55% R_{CP} nuclear modification factors. At low-p_T R_{CP} scales with the number of participants for all particles except the $\overline{\Lambda}$. With increasing p_T, K^0_S mesons reach values of $R_{\mathrm{CP}} \approx 1$; we did not observe the enhancement
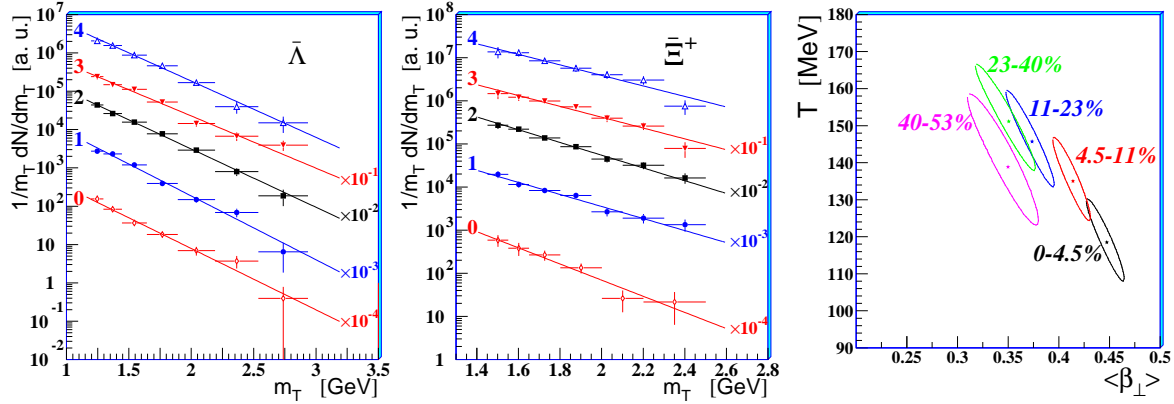
Figure 3. Transverse mass spectra for $\overline{\Lambda}$ (left panel) and $\overline{\Xi}^+$ (middle pannel) from Pb–Pb collisions at 158 A GeV/c for different centralities. Class 4, displayed uppermost, corresponds to the most central collisions (5%); class 0, displayed lowermost, corresponds to the most peripheral ones(40–53%). Right: 1σ confidence level contours from fits of all strange particle spectra for different centrality classes.

above unity that was measured in proton–nucleus relative to pp collisions (Cronin effect [20]). An enhancement is, instead, observed for strange baryons, Λ and $\overline{\Lambda}$, that reach $R_{CP} \simeq 1.5$ at $p_T \simeq 3$ GeV/c. In fig. 4 (middle panel) we compare our K_S^0 data
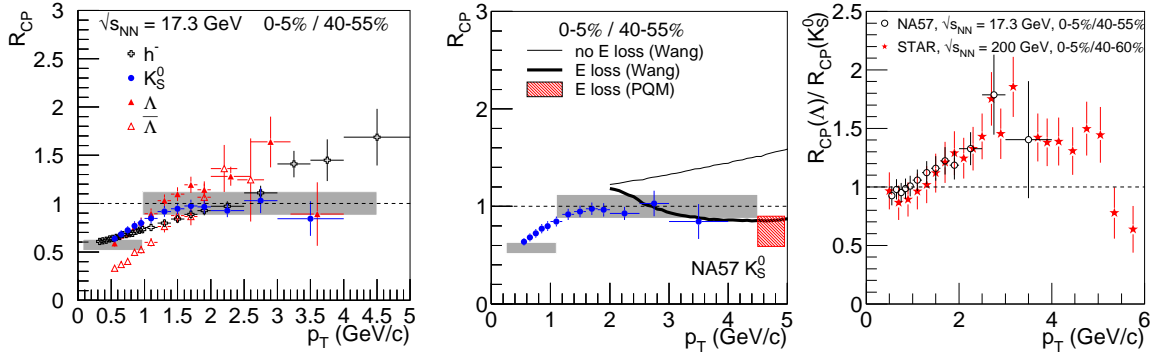

Figure 4. Left: R_{CP} ratios for negatively charged particles (h^-) and singly-strange particles in Pb–Pb collisions at $\sqrt{s_{NN}} = 17.3$ GeV [19]. The width of the shaded band centered at $R_{CP} = 1$ indicates the systematic error due to the uncertainty on the values of $\langle N_{coll} \rangle$ in each class; the band at low p_T show the value expected for scaling with the number of participants. Middle: K_S^0 $R_{CP}(p_T)$ compared to predictions [21, 22] with and without energy loss. Right: ratio of Λ R_{CP} to K_S^0 R_{CP}, as a function of p_T, at the SPS (NA57 at $\sqrt{s_{NN}} = 17.3$ GeV) and at RHIC (STAR at $\sqrt{s_{NN}} = 200$ GeV [17]).

with predictions obtained from a pQCD-based calculation [21], including (thick line) or excluding (thin line) in-medium parton energy loss. The initial gluon rapidity density of the medium was scaled down from that needed to describe RHIC data, according to the decrease by about a factor 2 in the charged particle multiplicity. The data are better described by the curve that includes energy loss. The prediction of a second model of parton energy loss (PQM) that describes several energy-loss-related observables at

RHIC energies [22] is also in agreement with the first model. Figure 4 (right panel) shows the ratio of Λ R_{CP} to K_S^0 R_{CP}, as measured from our data and by STAR at $\sqrt{s_{NN}} = 200$ GeV [17] (note that the sum $\Lambda + \overline{\Lambda}$ is shown for STAR results). The similarity of the Λ–K pattern to that observed at RHIC can be taken as an indication for coalescence effects [23] at SPS energy.

6. Conclusions

The planned experimental programme of NA57 has been succesfully carried through. The experiment has made several substantial contributions to the study of the properties of the new state formed in heavy-ion collisions at the SPS, particularly in three areas: the study of the hyperon enhancements and of their dependence on strangeness content, collision centrality and collision energy; the study of the transverse expansion and freeze-out conditions, and in particular their centrality and energy dependence; the study of the nuclear modification factors at the SPS.

References

[1] Caliandro R *et al* 1996 CERN/SPSLC 96-40 SPSLC/P300 (*"NA57 Proposal"*)
[2] Andersen E (WA97 Collaboration) *et al.* 1999 *Phys. Lett.* B **449** 401
    Antinori F (WA97 Collaboration) *et al.* 1999 *Nucl. Phys.* A **661** 130c
[3] Heinz U and Jacob M 2000 *Preprint* nucl-th/0002042 and reference therein
[4] Antinori F *et al.* (NA57 Collaboration) 2006 *J. Phys. G: Nucl. Part. Phys.* **32** 427
[5] Antinori F *et al.* (NA57 Collaboration) 2005 *J. Phys. G: Nucl. Part. Phys.* **31** 321
[6] Rafelski J and Müller B 1982 *Phys. Rev. Lett.* **48** 1066; ibidem 1986 *Phys. Rev. Lett.* **56** 2334
    Koch P, Müller B and Rafelski J 1986 *Phys. Rep.* **142** 167; Rafelski J 1991 *Phys. Lett.* B **262** 333
[7] Bruno G E *et al* (NA57 Collaboration) 2004 *J. Phys. G: Nucl. Part. Phys.* **30** s717
[8] Antinori F *et al* (NA57 Collaboration) 2005 *J. Phys. G: Nucl. Part. Phys.* **31** 1345
[9] Blume C *et al* (NA49 Collaboration) these proceedings
[10] Barnby L *et al* (STAR Collaboration) these proceedings
[11] Tounsi A *et al* 2003 *Nucl. Phys.* A **715** 565c
[12] Antinori F *et al.* (NA57 Collaboration) 2004 *J. Phys. G: Nucl. Part. Phys.* **30** 823
[13] Antinori F *et al.* (NA57 Collaboration) 2006 *J. Phys. G: Nucl. Part. Phys.* **32** 2065
[14] Schnedermann E, Sollfrank J and Heinz U 1993 *Phys. Rev.* C **48** 2462
    Schnedermann E and Heinz U 1994 *Phys. Rev.* C **50** 1675
[15] Van Leeuwen M *et al.* (NA49 Collaboration) 2003 *Nucl. Phys.* A **715** 165
    Friese V *et al.* (NA49 Collaboration) 2004 *J. Phys. G: Nucl. Part. Phys.* **30** S119
[16] Bruno G E *et al* (NA57 Collaboration) 2005 *J. Phys. G: Nucl. Part. Phys.* **31** S127
[17] Adams J *et al.* (STAR Collaboration) 2004 *Phys. Rev. Lett.* **92** 052302
[18] Aggarwal M M *et al.* (WA98 Collaboration) 2002 *Eur. Phys. J.* C **23** 225; d'Enterria D 2004 *Phys. Lett.* B **596** 32; Reygers K *et al* (WA98 Collaboration) 2007 *J. Phys. G: Nucl. Part. Phys.* S797.
[19] Antinori F *et al.* 2005 *Phys. Lett.* B **623** 17
[20] Cronin J *et al.* 1975 *Phys. Rev.* D **11** 3105.
[21] Wang X N 2000 *Phys. Rev.* C **C61** 064910; private communication.
[22] A. Dainese *et al.*, *Eur. Phys. J.* **C38** (2005) 461; private communication.
[23] Hwa R C and Yang C B 2003 *Phys. Rev.* C **67** 064902; Fries R J *et al.* 2003 *Phys. Rev.* C **68** 044902; Greco V *et al.* *Phys. Rev.* C **68** 034904.